

Structural Modifications Induced by High-Temperature Quenching Treatments in the Fast Ion Conductor $\text{Li}_{0.18}\text{La}_{0.61}\text{TiO}_3$: A Neutron Diffraction Study

A. Varez,[†] Y. Inaguma,[‡] M. T. Fernández-Díaz,[§] J. A. Alonso,^{||} and J. Sanz^{*,||}

Department of Material Science and Engineering, Universidad Carlos III de Madrid, E-28911, Leganés, Spain, Department of Chemistry, Gakushuin University, Tokyo 171-8588, Japan, Institut Laue-Langevin, F-38045, Grenoble, France, and Instituto de Ciencia de Materiales, CSIC, Cantoblanco, E-28049, Madrid, Spain

Received June 2, 2003. Revised Manuscript Received September 10, 2003

The crystal structure of the fast ionic conductor $\text{Li}_{0.18}\text{La}_{0.61}\text{TiO}_3$ perovskite-type was determined at 5 K by neutron diffraction (ND) experiments in samples cooled slowly and quenched from 1600 K. In both cases, the perovskite displayed superstructures of the elementary perovskite. In the slowly cooled sample, a $2a_p, 2a_p, 2a_p$ superstructure with orthorhombic symmetry was detected ($Cmmm$ space group). The main characteristics of this structure are the out-of-phase tilting of TiO_6 octahedra in the [010] direction, and the ordering of La vacancies in alternate planes along the c -axis. In samples quenched in liquid nitrogen from high temperature, La and vacancies become disordered and the structure adopts a rhombohedral $\sqrt{2}a_p, \sqrt{2}a_p, 2\sqrt{3}a_p$ symmetry ($R\bar{3}c$ space group). In this structure the octahedral tilting is produced along the three crystallographic axes as a consequence of the disordered arrangement of the La and the vacancies. A detailed analysis of Fourier difference maps in both samples revealed the preference of Li for the 4-fold coordination at the center of square windows that connect contiguous A-sites of the perovskite.

Introduction

Interest in $\text{Li}_{3-x}\text{La}_{2/3-x}\text{TiO}_3$ perovskites ($0 < x < 0.17$) has grown since the discovery of its high ionic conductivity ($10^{-3} \Omega^{-1}\text{cm}^{-1}$ at $T = 300$ K).^{1,2} Considerable efforts have been devoted to determining the structural characteristics that enhance Li mobility, such as Li coordination, structural network distortions, vacant site distribution, etc. In Li-poor perovskites, the ordering of La vacancies is produced in alternate planes along the c -axis, favoring a two-dimensional Li conductivity, whereas in Li-rich samples, the ordering of vacant sites is eliminated and conductivity becomes three-dimensional. To reduce cation ordering in perovskites, Harada et al.³ studied the influence of quenching treatments and showed that the quenching from 1600 K into liquid N_2 stabilized the simplest cubic phase, with La and vacancies randomly distributed in A-sites of the perovskite.

A knowledge of the structure of these perovskites is required to explain Li ion mobility within the La–Ti–O framework. In particular, the tilting of the TiO_6 octa-

hedra introduces structural distortions in the square windows that connect contiguous A-sites, which could greatly affect Li mobility in perovskites. However, a precise determination of the perovskite structure by X-ray diffraction is difficult because of the weakness of reflections associated with small displacements of the oxygen atoms. This makes the neutron diffraction (ND) study of the tilting of the TiO_6 octahedra more suitable for this investigation.

In recent studies, the neutron diffraction technique has been used to determine the tilt of the TiO_6 octahedra in Li-poor $\text{Li}_{3-x}\text{La}_{2/3-x}\text{TiO}_3$ ($x = 0.04$ and 0.06) perovskites, described with the orthorhombic $Cm2m$ and $Cmmm$ space groups,^{4,5} and in the Li-rich end member $\text{Li}_{0.5}\text{La}_{0.5}\text{TiO}_3$, described with the rhombohedral $R\bar{3}c$ space group.⁶ In the first case, it was shown that a considerable distortion in TiO_6 octahedra was produced by ordering of La vacancies in alternate planes along the c -axis. In the second case, the octahedra become regular and the distribution of vacancy was disordered. A detailed analysis of Fourier map differences of the rhombohedral phase showed that Li cations occupy the center of the unit cell faces of the perovskite.⁶ This increases the number of vacant A-sites in conduction networks, and promotes Li mobility in this series of perovskites.⁷

* To whom correspondence may be addressed. E-mail: jsanz@icmm.csic.es.

[†] Universidad Carlos III de Madrid.

[‡] Gakushuin University.

[§] Institut Laue-Langevin.

^{||} Instituto de Ciencia de Materiales, CSIC.

(1) Belous, A. G.; Novitskaya, G. N.; Polyantetskaya, S. V.; Gornikov, Y. I. *Zh. Neorg. Khim.* **1987**, *32*, 283.

(2) Inaguma, Y.; Chen, L.; Itoh, M.; Nakamura, T.; Uchida, T.; Ikuta, H.; Wakihara, M. *Solid State Commun.* **1993**, *86*, 689.

(3) Harada, Y.; Ishigaki, T.; Kawai, H.; J. Kuwano. *Solid State Ionics* **1998**, *108*, 407. Inaguma, Y.; Katsumata, T.; Yu, J.; Itoh, M. *Mater. Res. Soc. Symp. Proc.* **1997**, *453*, 623

(4) Inaguma, Y.; Katsumata, T.; Itoh, M.; Y. Morii. *J. Solid. State Chem.* **2002**, *166*, 67.

(5) Sanz, J.; Alonso, J. A.; Várez, A.; Fernández-Díaz, M. T. *Dalton Trans.* **2002**, 1406–1408.

(6) Alonso, J. A.; Sanz, J.; Santamaría, J.; León, C.; Várez, A. M.; Fernández-Díaz, T. *Angew. Chem., Int. Ed.* **2000**, *3*, 619.

In this paper, structural changes produced during the thermal treatment of the Li-poor perovskite $\text{Li}_{0.18}\text{La}_{0.61}\text{TiO}_3$, are examined by neutron diffraction. Special efforts are made to define the tilting of TiO_6 octahedra and to localize Li ions at 5 K in slowly cooled and fast quenched samples by Fourier difference maps of neutron diffraction data.

Experimental Section

The $\text{Li}_{0.18}\text{La}_{0.61}\text{TiO}_3$ sample was prepared in polycrystalline form by solid state reaction of a stoichiometric mixture of high-purity previously dried Li_2CO_3 , La_2O_3 , and TiO_2 reagents.^{2,8,9} The reacted powder was pelletized and fired at 1573 K in air for 6 h using alumina crucibles. From 1600 K, samples were either quenched in liquid nitrogen (Q sample) or cooled slowly (1 °C/min) to room temperature (SC sample). The metal molar ratio was determined by inductively coupled plasma spectroscopy (ICP) using a JY-70 plus spectrometer. Purity of the phases was assessed from the analysis of X-ray powder diffraction patterns recorded between 13 and 70° using a Phillips X-pert diffractometer with ($\theta/2\theta$) Bragg–Brentano geometry and $\text{Cu K}\alpha$ radiation ($\lambda = 1.5418 \text{ \AA}$).

To reduce the absorption cross section in the neutron diffraction experiments, ⁷Li-enriched samples were prepared. ND patterns were collected at 5 K in the high-resolution D2B diffractometer at ILL-Grenoble. A wavelength of 1.594 Å was selected from a Ge monochromator. The counting time was 4 h, using about 4 g of sample contained in a vanadium can. For Rietveld structural analysis, data were collected between $2\theta = 5$ and 150°, by 0.02° steps. The FULLPROF program was used for the structural refinement. A pseudo-Voigt function was chosen to reproduce the line shape of diffraction peaks. In these analyses, the coherent lengths for La, Li, Ti, and O were 8.24, -1.90, -3.44, and 5.80 fm.

Results

The XRD patterns of the quenched and the slowly cooled samples were characteristic of single (a_p, a_p, a_p) cubic⁹ and c -axis doubled ($a_p, a_p, 2a_p$) orthorhombic¹⁰ perovskites. No extra peaks associated with impurities were detected. Unit cell parameters of both phases were 3.871 Å for the cubic perovskite and 3.859, 3.869, and 7.773 Å for the orthorhombic phase.

Figure 1 shows the ND patterns of the quenched and slowly cooled $\text{Li}_{0.18}\text{La}_{0.61}\text{TiO}_3$ perovskite recorded at 5 K. In both cases, the unit cell deduced from ND patterns differs from that deduced from XRD patterns. In the slowly cooled sample, the ($a_p, a_p, 2a_p$) unit cell deduced from XRD analysis^{9,11} does not reproduce all the peaks, and a larger unit cell is required. The so-called diagonal perovskite ($\sqrt{2}a_p, \sqrt{2}a_p, 2a_p$) with space groups $P4/mmm$,⁸ $Pmmm$,¹⁰ $Pban$,¹² and $P2/n$ were also tested. Although most of these models reproduced superstructure peaks, agreement factors obtained in Rietveld refinements were poor. The best refinement was obtained by using an orthorhombic ($2a_p, 2a_p, 2a_p$) unit cell,

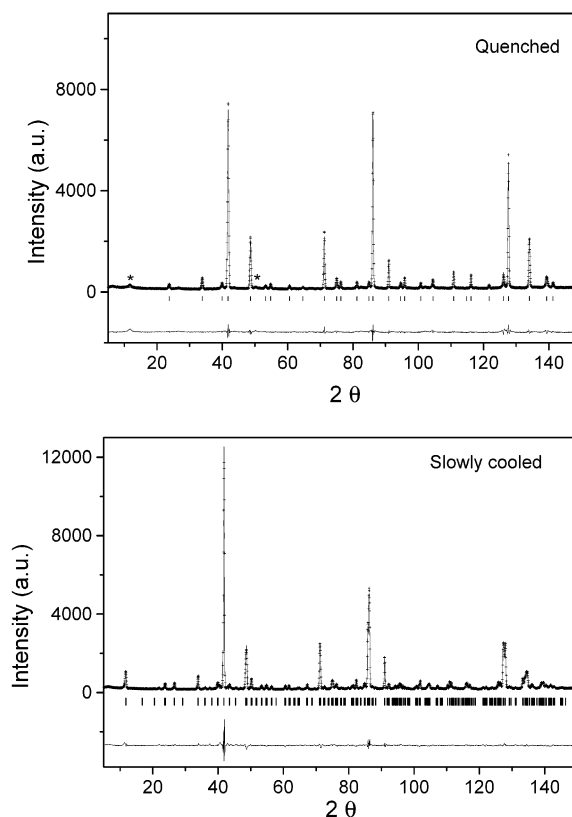


Figure 1. ND profiles recorded at 5 K on the slowly cooled and the quenched $\text{Li}_{0.18}\text{La}_{0.61}\text{TiO}_3$ perovskite. The dotted line marks experimental points and the solid line is the calculated profile. The lower trace shows the difference curve, and ticks denote expected peak positions. The influence of vacancy distribution on peaks intensity is clear. Small peaks labeled with asterisks correspond to the residual La-vacancy ordering of the slowly cooled sample.

with $Cmmm^4$ and $Cm2m^5$ space groups. Finally, the higher symmetry model was retained.

In the case of the quenched sample, the ND pattern was indexed with the rhombohedral $\sqrt{2}a_p, \sqrt{2}a_p, 2\sqrt{3}a_p$ unit cell⁶ (Figure 1). In this pattern, broad and small peaks (marked with asterisk) of the orthorhombic phase were still detected, indicating that full disordering of La and vacancies is difficult to achieve.

In two phases, deduced thermal factors of La, Ti, and O are all reasonable, and the cation stoichiometry deduced from occupancy factors is close to the chemical formula. The structural data deduced in orthorhombic and rhombohedral phases are given in Table 1.

Discussion

Depending on the thermal treatments used, two different phases were obtained in the $\text{Li}_{0.18}\text{La}_{0.61}\text{TiO}_3$ perovskite. In both cases, unit-cell parameters deduced from ND patterns were larger than those deduced from XRD patterns. Taking into account that superstructure peaks detected in ND patterns are produced by the tilting of octahedra, the Rietveld analysis of ND patterns was undertaken. Structural parameters deduced from the refinement of the two phases are summarized in Tables 1 and 2.

La-Vacancy Ordering. In the slowly cooled sample, an orthorhombic $2a_p, 2a_p, 2a_p$ unit cell was deduced from ND patterns. The structure of this phase was described

(7) Rivera, A.; León, C.; Santamaría, J.; Várez, A.; Vyunov, O.; Belous, A. G.; Alonso, J. A.; Sanz, J. *Chem. Mater.* **2002**, *14*, 5148.

(8) Várez, A.; García-Alvarado, F.; Morán, E.; Alario-Franco, M. A. *J. Solid State Chem.* **1995**, *118*, 78.

(9) Ibarra, J.; Várez, A.; León, C.; Santamaría, J.; Torres-Martínez, L. M.; Sanz, J. *Solid State Ionics* **2000**, *134*, 219.

(10) Paris, M. A.; Sanz, J.; León, C.; J.; Santamaría, Ibarra, J.; Várez, A. *Chem. Mater.* **2000**, *12*, 1694.

(11) Fourquet, J. L.; Duroy, H.; Crosnier-López, M. P.; *J. Solid State Chem.* **1996**, *127*, 283.

(12) MacEachern, M. J.; Dabkowska, H.; Garrett, J. D.; Amow, G.; Gong, W.; Liu, G.; Greedan, J. E. *Chem. Mater.* **1994**, *6*, 2092.

Table 1. Structural Parameters of $\text{Li}_{0.18}\text{La}_{0.61}\text{TiO}_3$ deduced from ND data recorded at 5 K

atom	position	x/a	y/b	z/c	B_{iso}	O_{cc}
Slowly cooled from 1600 K ^a						
La1	4i	0	0.2538(5)	0	0.22(2)	0.962 (3)
La2	4j	0	0.2595(8)	1/2	0.22(2)	0.258 (3)
Li1	8n	0	0.27(1)	0.236(8)	2.0(8)	0.11(3)
Li2	4f	1/4	1/4	1/2	2.0(8)	0.14(3)
Ti	8o	0.2474(6)	0	0.2599(4)	0.46(4)	1
O1	4g	0.2725(5)	0	0	0.79(6)	1
O2	4k	0	0	0.2133(4)	0.64(6)	1
O3	4l	0	1/2	0.2614(4)	0.96(7)	1
O4	8m	1/4	1/4	0.2337(4)	1.00(4)	1
O5	4h	0.2314(6)	0	1/2	1.09(6)	1
Quenched from 1600 K into liquid N ₂ ^b						
La	6a	0	0	1/4	0.14(8)	0.58 (2)
Li	18d	1/2	0	0	0.9(5)	0.05 (1)
Ti	6b	0	0	0	0.8(1)	1
O1	18e	0.5258(6)	0	1/4	^c	1

^a Space group $Cm\bar{m}m$ (65). $a = 7.7179(1)$, $b = 7.7397(1)$, $c = 7.7712(1)$ Å. Agreement factors: $R_1 = 5.83$, $R_F = 7.16$, $R_P = 4.90$, $R_{\text{WP}} = 6.85$, $R_{\text{exp}} = 2.67$; $\chi^2 = 6.48$. Li and La occupancy were constrained separately according to the chemical composition. ^b Space group $R\bar{3}c$ (167). $a = b = 5.4750(3)$, $c = 13.4106(8)$ Å. Agreement factors: $R_1 = 2.63$, $R_F = 2.73$, $R_P = 4.97$, $R_{\text{WP}} = 7.12$, $R_{\text{exp}} = 2.29$; $\chi^2 = 6.74$. ^c Anisotropic thermal factors: $\beta_{11} = 0.024(3)$, $\beta_{22} = 0.019(4)$, $\beta_{33} = 0.0003(3)$, $\beta_{12} = 0.010(4)$, $\beta_{13} = -0.0019(7)$, $\beta_{23} = -0.0035(7)$.

Table 2. Main Interatomic Distances (Å) and Angles (°) in the Two Phases of $\text{Li}_{0.18}\text{La}_{0.61}\text{TiO}_3$.

bond/angle	orthorhombic	rhombohedral
Ti–O1	2.028 (3)	1.941 (2) [$\times 6$]
Ti–O2	1.949 (9)	
Ti–O3	1.943 (9)	
Ti–O4	1.946 (4) [$\times 2$]	
Ti–O5	1.870 (3)	
<Ti–O>	1.947 (5)	1.941 (2)
La1–O1	2.877 (4) [$\times 2$]	2.595 (3) [$\times 3$]
La1–O1'	2.592 (4) [$\times 2$]	2.880 (3) [$\times 3$]
La1–O1''		2.741 (1) [$\times 6$]
La1–O2	2.571 (4) [$\times 2$]	
La1–O3	2.785 (4) [$\times 2$]	
La1–O4	2.648 (2) [$\times 4$]	
<La1–O>	2.687 (4)	2.7393 (2)
La2–O2	2.994 (9) [$\times 2$]	
La2–O3	2.632 (9) [$\times 2$]	
La2–O4	2.832 (2) [$\times 4$]	
La2–O5	2.686 (9) [$\times 2$]	
La2–O5'	2.788 (9) [$\times 2$]	
<La2–O>	2.794 (8)	
<O5–Ti–O _E > ^a	95.6 (3)	90.16(8)
<O1–Ti–O _E >	84.4 (3)	
<O _E –Ti–O _E >	89.3 (3)	
<Ti–O _E –Ti>	168.6(6)	171.6(1)
O1–Ti–O5	178.6(7)	180

^a O_E denotes equatorial oxygens in TiO₆ octahedra.

with the $Cm\bar{m}m$ ⁴ space group. A view of the crystal structure is given in Figure 2. In this model (Table 1a), La ions preferentially occupy La1 crystallographic sites at $z/c = 0$ planes, and the remaining lanthanum and vacancies are accommodated at the La2 site in $z/c = 0.5$ planes. The different occupation of alternating $z/c = 0$ and 0.5 planes by lanthanum is responsible for the c -axis doubling.

As a consequence of the La arrangement in the orthorhombic phase, Ti atoms are shifted from the center of the octahedra toward the vacancy-rich plane ($z/c = 0.5$) to compensate the asymmetric distribution of charges.^{9,11} This produces a significant distortion of the octahedra, with two different Ti–O distances along the c -axis, 1.870 and 2.028 Å, and four distances close to 1.947 Å in the ab plane (Table 2). This shift produces also different O1–Ti–O_E and O5–Ti–O_E angles (84.4 and 95.6°) in the octahedra which are compatible with a tetragonal $P4/m\bar{m}m$ distortion of the perovskite. However, the antiphase tilting of TiO₆ octahedra along

the b -axis reduced the symmetry of the perovskite to orthorhombic; (0 ϕ 0) model in the Glazer notation.¹³

In the quenched sample, a rhombohedral $R\bar{3}c$ symmetry with a $\sqrt{2}a_p, \sqrt{2}a_p, 2\sqrt{3}a_p$ unit cell was deduced, in which lanthanum and vacancy are randomly distributed in a single A-site. Structural features deduced in this sample are similar to those deduced in the quenched Li-rich perovskite $\text{Li}_{0.5}\text{La}_{0.5}\text{TiO}_3$ ⁶ (Figure 2). Oxygen thermal factors were anisotropically refined, with the short axis of the thermal ellipsoid disposed in the covalent Ti–O–Ti direction. Parameters deduced in the refinement are given in Table 1b. TiO₆ octahedra are regular (Ti–O distances ~ 1.941 Å) and octahedral tilting is produced along three axes, (a[−] a[−] a[−] model in Glazer notation).

Square Windows Geometry. In slowly cooled and quenched samples, the mean La–O distances are basically the same (2.738 Å) but the La-vacancy ordering in alternating planes produces the differentiation of two sites for La cations. In La-rich planes, the mean La2–O distance is longer than that in La-poor planes (<La2–O> = 2.794 Å; <La1–O> = 2.687 Å).

In these perovskites the coordination of lanthanum cations is affected by the octahedral tilting. As a consequence of different tilting schemes, La–O distances are considerably different in the two phases. In the quenched sample, the octahedral tilting in three directions of the perovskite produces a distorted coordination of La cations (2.59–2.88 Å). In the case of the orthorhombic sample, the octahedral tilting along the b -axis produces a coordination of La2 (La2–O = 2.63–2.99 Å) more distorted than that of the La1 atom (La1–O = 2.57–2.88 Å).

A closer analysis of the two structures showed the presence of several square windows that connect contiguous A-sites in the perovskite. The number and dimensions of the oxygen square windows differed along the three axes (Figure 2). In the orthorhombic sample, diagonal distances along the a -axis are larger (3.880–4.145 Å) than those along the b - and c -axes (3.59–4.45 Å for b ; 3.86–3.89 Å for c -axis), consequently Li mobility should be favored along the a -axis. This supports the

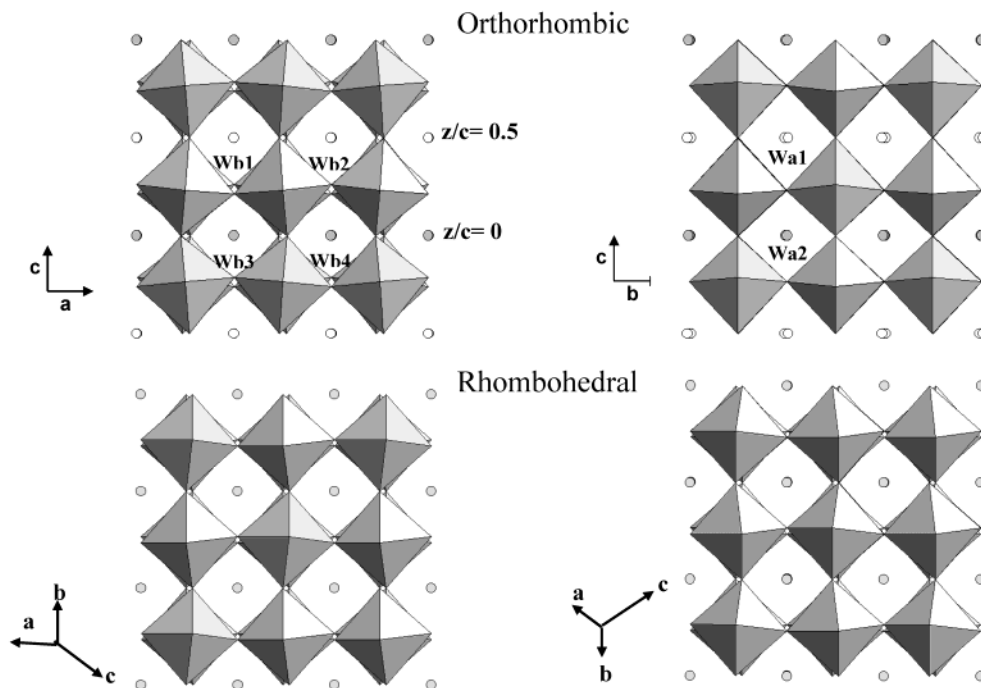


Figure 2. Structural views of the orthorhombic (top) and rhombohedral (bottom) phases of the $\text{Li}_{0.18}\text{La}_{0.61}\text{TiO}_3$, illustrating square windows in the [010] and [100] directions of the ideal perovskite. Octahedral tilting and differences in La coordination in $z/c = 0$ (fully occupied) and 0.5 (partially occupied) planes are illustrated.

low dimensionality deduced for Li motion from NMR experiments.^{10,14} In the case of the rhombohedral phase, all the square windows are identical, which supports the onset of a three-dimensional Li motion. However, distortions produced in square windows are important (diagonal distances = 3.67–4.08 Å) and allow us to explain the decrease observed in the conductivity of the Li-poor samples after quenching treatments.^{3,15}

Li Sites. To localize the Li ions we performed Fourier maps of differences between observed and calculated structure factors. Calculated factors were obtained considering only La, Ti, and O atoms in the perovskite. The negative scattering length of Li favors this analysis. Fourier maps obtained on different planes perpendicular to the c -axis of the orthorhombic phase showed small negative peaks in $z/c = 0, 0.25,$ and 0.5 planes (Figure 3). Some of them were rejected because of their unrealistic positions (0.06,0.35,0) or unreasonable Li–O distances (0.2, 0.05, 0). In the quenched sample, peaks of negative intensity were located in the $z/c = 0$ Fourier section at $(1/2,0,0)$ sites of the rhombohedral unit cell (Figure 4).

It is interesting to note that all the reported sites correspond to positions at the center of unit cell faces of the ideal perovskite, with Li–O distances of 1.81 and 2.07 Å. In these positions, Li ions are surrounded by four oxygens and two sites that could be occupied by La, Li, or vacancies. From electrostatic considerations, the most stable configuration of lithium is that surrounded by four oxygens and two vacant A-sites. This configuration is favored in planes $z/c = 0.5$ of the orthorhombic phase and in a large number of square windows of the rhombohedral phase. It must be remem-

bered that the number of vacant A-sites increases as a consequence of the occupation of unit cell faces of the perovskite by lithium.⁶

A similar Li 4-fold coordination has been deduced by neutron powder diffraction in the low-temperature phases of NASICON compounds with Li–O distances between 1.8 and 2.1 Å. In these samples a triclinic–rhombohedral transition takes place improving considerably the Li mobility.^{16–18} To determine the occupancy of deduced sites, the Rietveld refinement of the orthorhombic phase was performed considering only one Li in each possible site deduced from the Fourier analysis. Positions considered at $z/c = 0.5$ (vacancy-rich plane) and $z/c = 0.25$ (Ti plane) improved the refinement. In the case of $z/c = 0$ (La-rich plane) only $4e$ sites gave reasonable R_1 values. At a second stage, we considered the simultaneous occupancy of the most realistic sites deduced in previous analyses. Occupancy factors of sites located at $z/c = 0$ ($4e$, $2a$, and $2b$) decreased considerably. In the $z/c = 0.5$ plane, the occupancy of $4f$ sites reached values close to 0.14, while that of $2c$ and $2d$ sites decreased to zero. Finally, in $8n$ sites at $z/c = 0.25$, values close to 0.11 were obtained. In all cases, the probability of finding two vacant A-sites at neighboring unit cells is high. The total amount of Li considered in this analysis was near that deduced from the chemical composition of the perovskite. The incorporation of Li atoms to the refinement improved the R_1 agreement factor from 6.7 to 5.8%, indicating that the Li distribution deduced is acceptable.

In the quenched phase, Li ions were randomly distributed at square windows that connect contiguous

(14) Rivera, A.; Leon, C.; J. Santamaría, Varez, A.; Paris, M. A.; Sanz, J. J. *Non-Cryst. Solids* **2002**, *307*, 992.

(15) Várez, A.; Ibarra, J.; Rivera, A.; León, C.; Santamaría, J.; Laguna, M. A.; Sanjuán, M. L.; Sanz, J. *Chem. Mater.* **2003**, *15*, 225.

(16) Morin, E.; Angenault, J.; Couturier, J. C.; Quarton, M.; He, H.; Klinowski, J. *Eur. J. Solid State Inorg. Chem.* **1997**, *34*, 947.

(17) Losilla, E. R.; Aranda, M. A. G.; Martínez-Lara, M.; Bruque, S. *Chem. Mater.* **1997**, *9*, 1678.

(18) Catti, H. Stramare, S.; Ibberson, R. *Solid State Ionics* **1999**, *123*, 173.

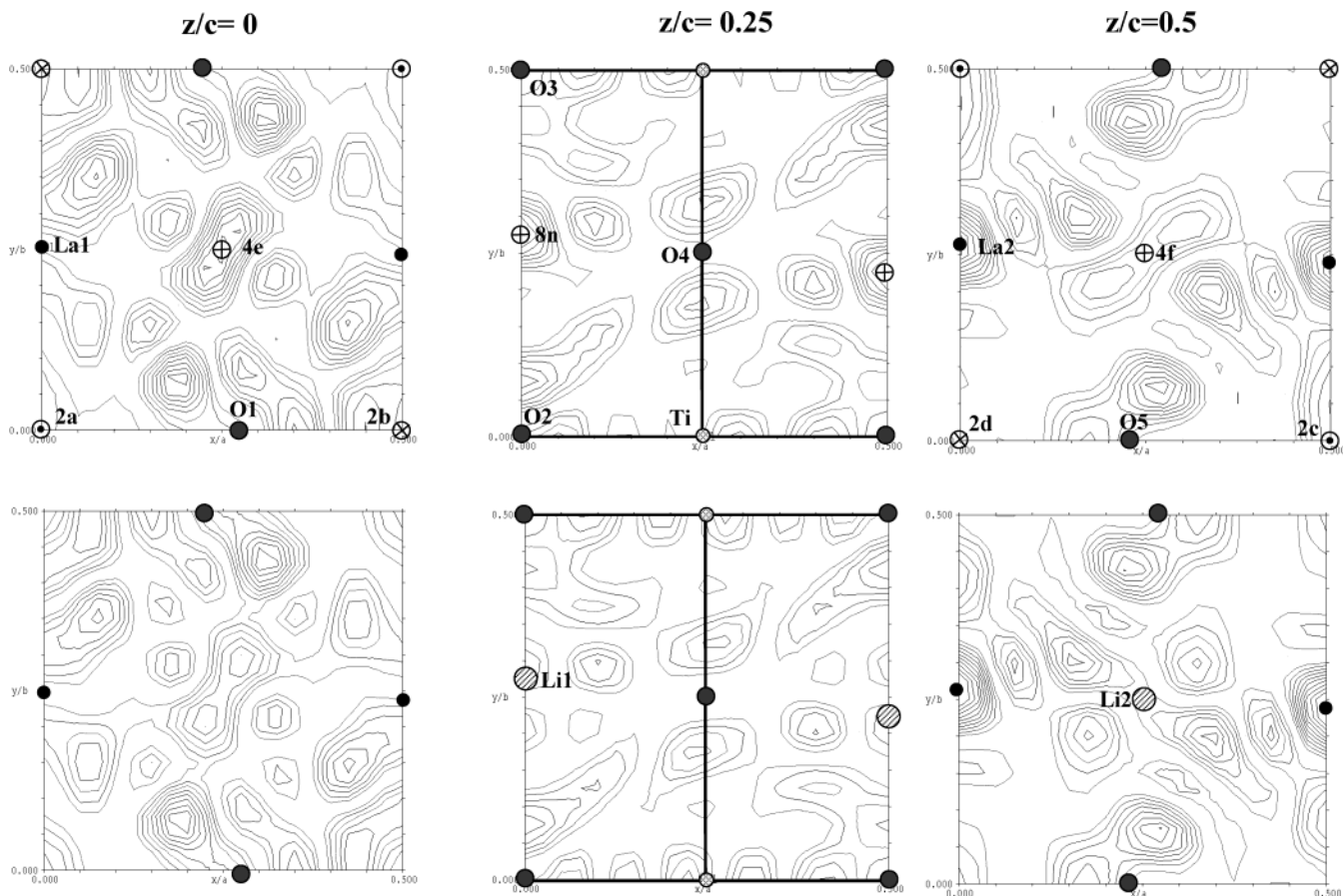


Figure 3. Difference Fourier maps for $z/c = 0, 0.25,$ and 0.5 planes in the slowly cooled $\text{Li}_{0.18}\text{La}_{0.61}\text{TiO}_3$ sample, before (top) and after (bottom) inclusion of Li ions in the refinement.

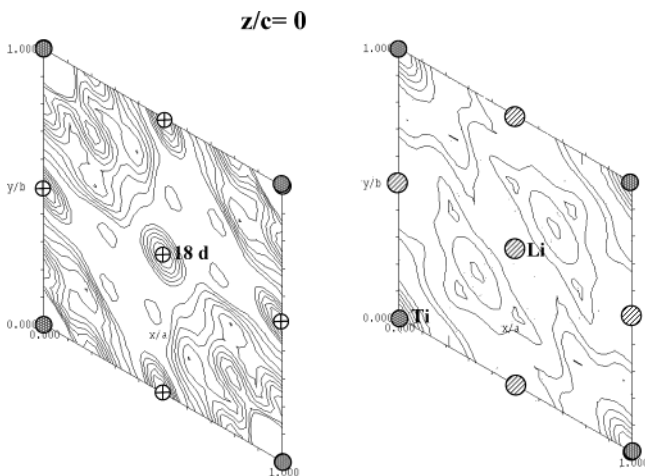


Figure 4. Difference Fourier maps for $z/c = 0$ plane of the quenched $\text{Li}_{0.18}\text{La}_{0.61}\text{TiO}_3$ perovskite, before (left) and after (right) inclusion of Li ions in the refinement.

A-sites. After the introduction of Li into the structural model, the refinement improved considerably (R_1 decreased from 4.5 to 2.7%) and minima disappeared from the Fourier map (Figure 4). This agrees with the results previously reported on the $\text{Li}_{0.5}\text{La}_{0.5}\text{TiO}_3$ sample.⁶

Concluding Remarks

ND structural analysis of the Li-poor $\text{Li}_{0.18}\text{La}_{0.61}\text{TiO}_3$ perovskite showed that vacancies are preferentially disposed in alternating planes in the slowly cooled

sample but are disordered in the quenched sample. In the low-temperature orthorhombic $2a_p, 2a_p, 2a_p$ phase, besides the La ordering along the c -axis, an out-of-phase tilting of octahedra was detected along the b -axis. The high-temperature phase adopted a rhombohedral symmetry in which La and vacancies became disordered and the same tilting of TiO_6 octahedra was produced along the three equivalent directions. In the slowly cooled sample, the octahedral tilting was described as $0\varphi 0$, but in the quenched samples it was $\varphi\varphi\varphi$ ($a^0b^-c^0$ and $a^-a^-a^-$ in Glazer's notation).¹³

Both structural features, namely the octahedral tilting and the vacancy distribution, are responsible for changes in the dimensionality of the Li motion. The two-dimensional lithium mobility detected in Li-poor members contrasts with the three-dimensional mobility favored in the quenched sample.^{14,15} In both samples, the location of Li ions at unit cell faces of the perovskite is produced, but the occupation of different square windows depends on the distribution of the La atoms in the perovskite. In general, the most favorable sites are those located between two vacant A-sites.

Acknowledgment. We thank M.L. Sanjuan, C. León, and J. Santamaría for helpful discussions and ILL for provision of neutron beam time. We thank also the Spanish CICYT for financial support (MAT2001-3713-C04-03 and MAT 2001-0539 projects).

CM030342E